

Discrete reduced-symmetry solitons and second-band vortices in two-dimensional nonlinear waveguide arrays

Magnus Johansson

Department of Physics, Chemistry and Biology, Linköping University, Sweden

Santiago, April 7, 2010

Magnus Johansson,^{1,2,3,*} Andrey A. Sukhorukov,^{1,†} and Yuri S. Kivshar^{1,‡}

¹*Nonlinear Physics Centre, Research School of Physics and Engineering, Australian National University, Canberra, Australian Capital Territory 0200, Australia*

²*Department of Physics, Chemistry and Biology (IFM), Linköping University, SE-581 83 Linköping, Sweden*

³*School of Pure and Applied Natural Sciences, University of Kalmar, SE-391 82 Kalmar, Sweden*

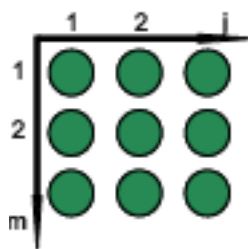
PHYSICAL REVIEW E **80**, 046604 (2009)

Aim: To describe dynamics of **nonlinear localized modes** in two-dimensional **periodic** structures, where each individual waveguide mode has a **dipolar** structure (“*p*-band modes”).

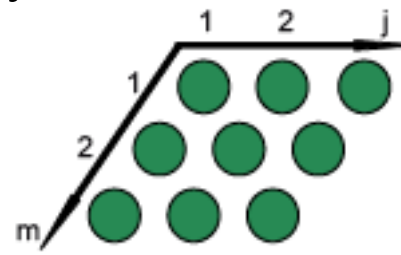
⇒ 2 orthogonal **degenerate** individual modes for uncoupled waveguides:



What kinds of **discrete** (“gap”) **solitons** may exist in different lattice types??



square ↔ triangular



Outline:

- Coupled-mode-approach → discrete equations for **two coupled fields** describing **degenerate** waveguide modes of **dipolar** character.
- Key feature: **anisotropic dispersion** yields solutions which break lattice rotational symmetry.
- Use standard machinery for discrete equations to obtain **strongly localized solutions**, and analyze their **stability** and **mobility**.
- Relate to recent experiments on “**reduced-symmetry gap solitons**” and “**second-band vortex lattice solitons**” in square and triangular lattices.
- Obtain conditions for **directional mobility** of dipole modes and predict **oscillatory instabilities** for vortex modes.
- Introduce concept of “**rotational Peierls-Nabarro barrier**”, defining the minimum energy needed for **rotation** of stable dipole modes.

cf. also a similar, very recent approach to describe quantum states of p-band bosons in optical lattices, in a mean-field model describing superfluid regime:

A. Collin, J. Larson, J.-P. Martikainen, PRA **81**, 023605 (2010)

Experimental motivations:

PRL 96, 023905 (2006)

PHYSICAL REVIEW LETTERS

Reduced-Symmetry Two-Dimensional Solitons in Photonic Lattices

Robert Fischer,¹ Denis Träger,^{1,2} Dragomir N. Neshev,¹ Andrey A. Sukhorukov,¹
Wieslaw Krolikowski,¹ Cornelia Denz,² and Yuri S. Kivshar¹

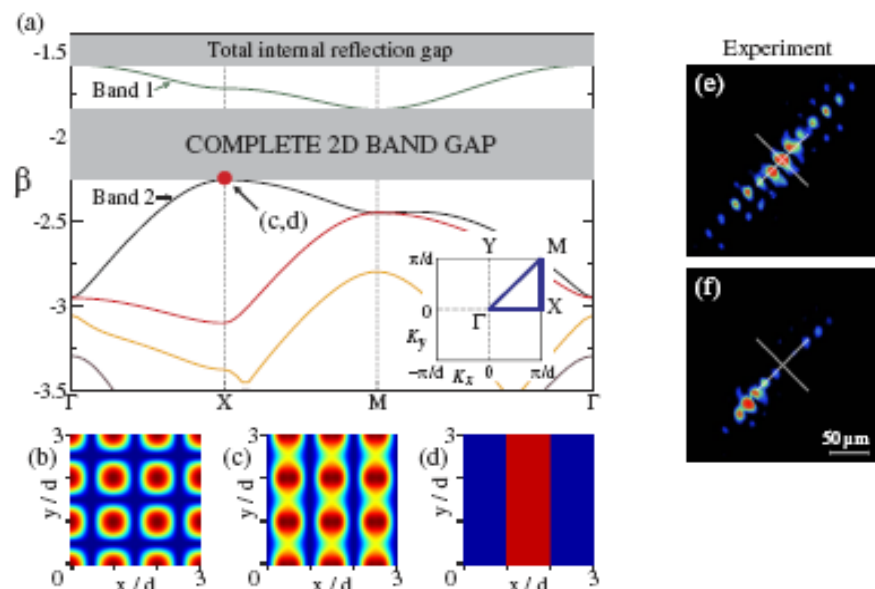


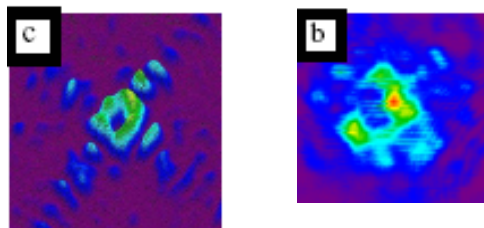
FIG. 1 (color online). (a), (b) Band gap spectrum and intensity distribution of the 2D square lattice. The horizontal axis in (a) corresponds to a contour shown in the inset. (c), (d) Calculated intensity and phase distribution of the Bloch wave from the X point of the second band of the spectrum (a).

PRL 95, 053904 (2005)

PHYSICAL REVIEW LETTERS

Observation of Second-Band Vortex Solitons in 2D Photonic Lattices

Guy Bartal,¹ Ofer Manela,¹ Oren Cohen,¹ Jason W. Fleischer,² and Mordechai Segev¹



Observation of nonlinear self-trapping in triangular photonic lattices

Christian R. Rosberg, Dragomir N. Neshev, Andrey A. Sukhorukov,
Wieslaw Krolikowski, and Yuri S. Kivshar

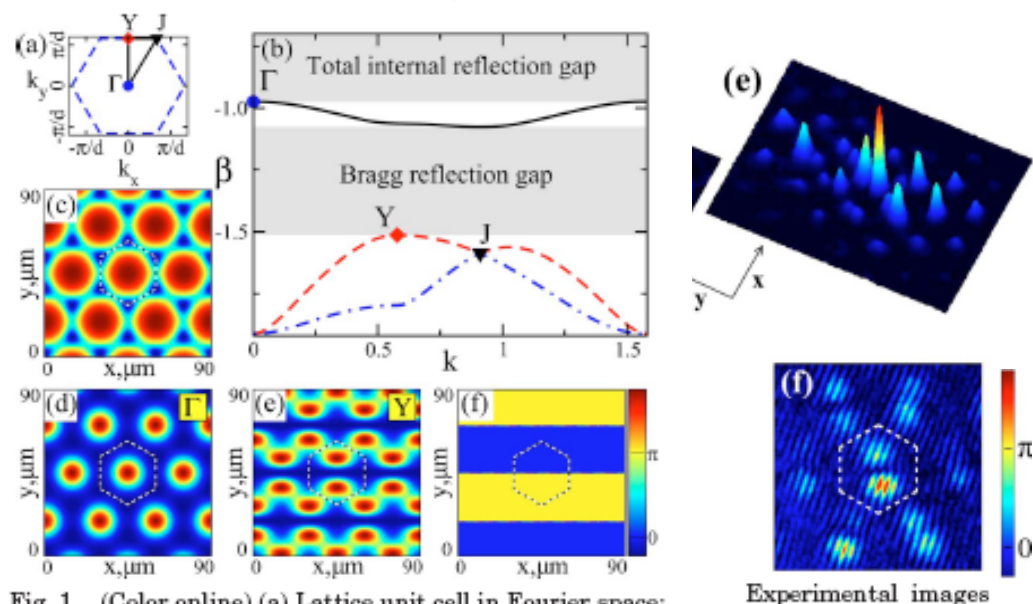


Fig. 1. (Color online) (a) Lattice unit cell in Fourier space; (b) Bloch-wave dispersion along the contour passing through the high-symmetry points marked in (a); (c) refractive index profile of the triangular lattice; (d), (e) Bloch waves corresponding to the Γ and Y points in (a) and (b); (d) intensity at the Γ point of the first band; (e), (f) intensity and phase at the Y point of the second band.

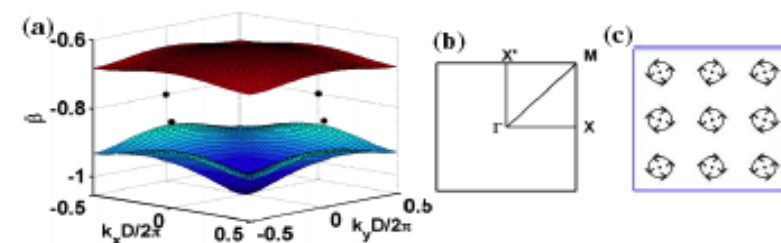


FIG. 1 (color online). (a) The first two bands of the band structure in a 2D square lattice with $D = 10$. The four thick dots mark the X-symmetry points. (b) High symmetry points of the reciprocal lattice. (c) Phase structure of a counterrotating vortex array, with the arrow in each vortex showing the direction of increasing phase.

Earlier theoretical predictions:

Based on approximation of **slowly varying envelopes** → justified only close to linear band, **weak discreteness**.

VOLUME 71, NUMBER 8

PHYSICAL REVIEW LETTERS

23 AUGUST 1993

Nonlinear Optical Solitary Waves in a Photonic Band Gap

Sajeev John and Neşet Aközbek

PHYSICAL REVIEW E

VOLUME 57, NUMBER 2

FEBRUARY 1998

Optical solitary waves in two- and three-dimensional nonlinear photonic band-gap structures

Neşet Aközbek and Sajeev John

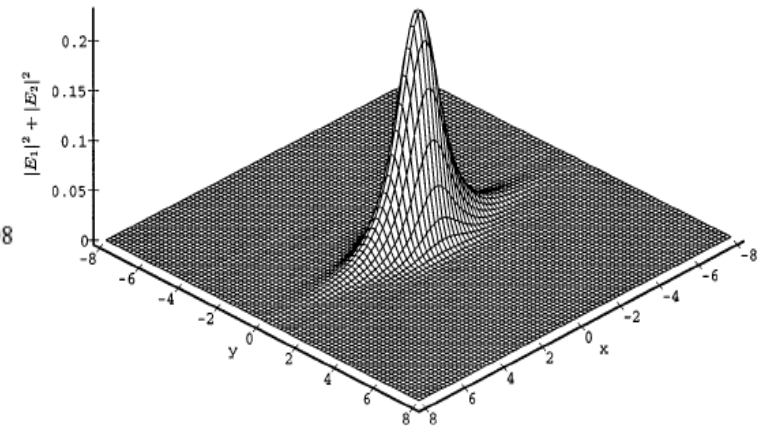


FIG. 11. Plotted is the energy density $(|E_1|^2 + |E_2|^2)$ (a.u.) of the X solitary wave using the numerical finite element method ($N=10$).

September 1, 2004 / Vol. 29, No. 17 / OPTICS LETTERS 2049

Two-dimensional higher-band vortex lattice solitons

Ofer Manela, Oren Cohen, Guy Bartal, Jason W. Fleischer, and Mordechai Segev

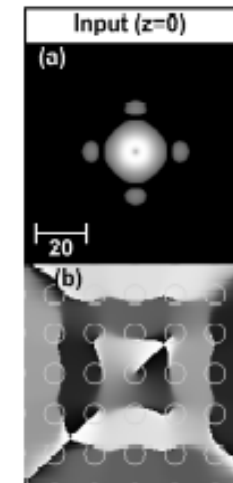
More recent work:

Shi/Yang, PRE **75**, 056602 (2007):

Numerical continuation of small-amplitude solutions from band edges into different families of solitary waves.

Dohnal, Pelinovsky, Schneider, J. Nonlinear Sci. **19**, 95 (2009):

Rigorous proof of persistence of localized gap solitons beyond small-amplitude limit, for separable potentials.



Strongly discrete system: coupled-mode equations

Consider single 2D waveguide with two orthogonal modes $\Psi_a(x, y)$ and $\Psi_b(x, y)$ with **same propagation constant** k :

$$-k\Psi_{a,b} + D \frac{\partial^2 \Psi_{a,b}}{\partial x^2} + D \frac{\partial^2 \Psi_{a,b}}{\partial y^2} + V(x, y)\Psi_{a,b} = 0$$

Lattice of coupled waveguides:

$$V = \sum_m V_s(x - x_m, y - y_m);$$

Express total field as sum of individual waveguide modes:

$$\Psi = \sum_m [A_m \Psi_a(x, y) + B_m \Psi_b(x, y)] \exp(ikz)$$

Assume weakly overlapping modes \rightarrow general set of coupled-mode equations:

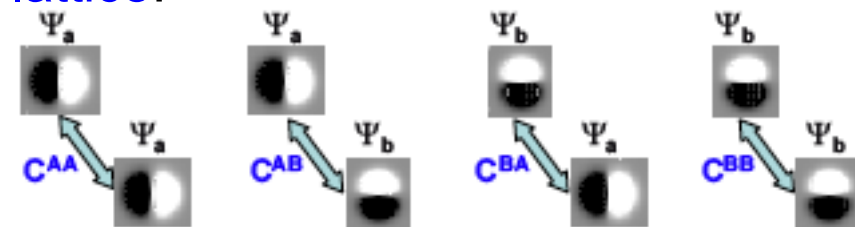
$$i \frac{dA_m}{dz} + \sum_j C_{m,j}^{AA} A_j + \sum_j C_{m,j}^{AB} B_j + \gamma_A |A_m|^2 A_m + \sigma (2|B_m|^2 A_m + B_m^2 A_m^*) = 0,$$

$$i \frac{dB_m}{dz} + \sum_j C_{m,j}^{BA} A_j + \sum_j C_{m,j}^{BB} B_j + \gamma_B |B_m|^2 B_m + \sigma (2|A_m|^2 B_m + A_m^2 B_m^*) = 0.$$

Parameters γ , σ determined by geometry of the **waveguides**.

Coupling constants C determined by geometry of the **lattice**:

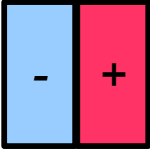
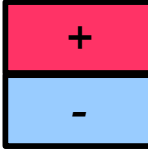
Assume **symmetric waveguides**: $\gamma_A = \gamma_B \equiv \gamma$



Single waveguide: all coupling parameters $C \equiv 0$ (“anticontinuous limit”)

Wish to describe solutions associated with 2nd dispersion band \rightarrow

assume modes with dipolar structure with nodelines through waveguide center:

ψ_a : horizontal dipole  , ψ_b vertical dipole 

There are three fundamental types of stationary solutions, and their stability is determined by ratio σ/γ (e.g. Kivshar/Agrawal, Optical Solitons, and references therein):

I. “Single-mode” (horizontal/vertical) dipoles:

$$A = \sqrt{\beta/\gamma} \exp(i\beta z), B = 0; \text{ or } A = 0, B = \sqrt{\beta/\gamma} \exp(i\beta z): \text{ stable for } 0 < \sigma/\gamma \leq 1/3$$

II. “Mixed-mode” (diagonal) dipoles: $A = \pm B = \sqrt{\beta/(\gamma + 3\sigma)} \exp(i\beta z)$ stable for $1/3 \leq \sigma/\gamma < 1$

III. Vortices: $A = \pm iB = \sqrt{\beta/(\gamma + \sigma)} \exp(i\beta z)$, stable for all $0 < \sigma/\gamma < 1$

Limit case of marginal stability $\sigma/\gamma = 1/3$ corresponds to circularly symmetric waveguide.

Weakly coupled waveguides (“continuation from anticontinuous limit”)

(Related approach used for “discrete vector solitons”, e.g.

Hudock et al., Phys. Rev. E **67**, 056618 (2003), Meier et al., Phys. Rev. Lett. **91**, 143907 (2003),

Horne et al, Phys. Rev. E **73**, 066601 (2006).)

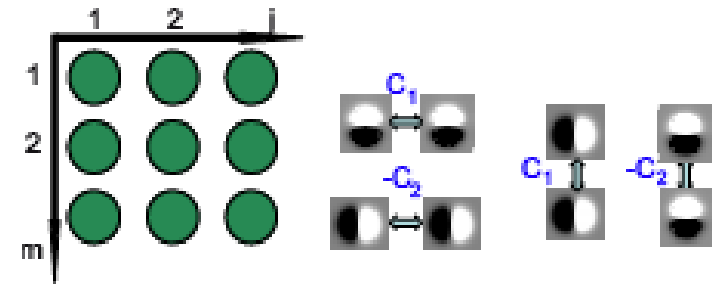
Square lattice with nearest-neighbour coupling: $(x, y) = (ja, ma)$.

$$i \frac{dA_{m,j}}{dz} + C_1(A_{m+1,j} + A_{m-1,j}) - C_2(A_{m,j+1} + A_{m,j-1}) + \gamma |A_{m,j}|^2 A_{m,j} + \sigma (2|B_{m,j}|^2 A_{m,j} + B_{m,j}^2 A_{m,j}^*) = 0$$

$$i \frac{dB_{m,j}}{dz} - C_2(B_{m+1,j} + B_{m-1,j}) + C_1(B_{m,j+1} + B_{m,j-1}) + \gamma |B_{m,j}|^2 B_{m,j} + \sigma (2|A_{m,j}|^2 B_{m,j} + A_{m,j}^2 B_{m,j}^*) = 0$$

$C_1, C_2 > 0$ $C_1 \neq C_2$ generally, due to

anisotropy of dipole waveguide modes:



Two conserved quantities:

Hamiltonian: $H = \sum_{m,j} \{ 2C_1 \Re(A_{m,j} A_{m+1,j}^* + B_{m,j} B_{m,j+1}^*) - 2C_2 \Re(A_{m,j} A_{m,j+1}^* + B_{m,j} B_{m+1,j}^*)$
 (energy) $+ \frac{\gamma}{2} (|A_{m,j}|^4 + |B_{m,j}|^4) + \sigma (2|A_{m,j}|^2 |B_{m,j}|^2 + \Re[A_{m,j}^2 B_{m,j}^{*2}]) \}$

Total power (norm): $P = \sum_{m,j} (|A_{m,j}|^2 + |B_{m,j}|^2)$

Numerical continuation from anticontinuous limit:

Existence: All three fundamental (**single-site**) stationary solutions may be continued smoothly for increasing coupling all the way to the **continuum limit**, where they approach standard **vector solitons**. (e.g., Kivshar/Agrawal and refs. therein)

Linear stability: Diagonalize $4N \times 4N$ matrix for N -site lattice.

(cf. Hudock et al., Phys. Rev. E **67**, 056618 (2003), Horne et al, Phys. Rev. E **73**, 066601 (2006))

1. $\sigma/\gamma \neq 1/3$: (non-circular waveguides)

- Dipole modes (I,II) **keep their stability properties** from anticontinuous limit.
- Vortex modes (III) are **stable** for weak coupling, but develop **oscillatory instabilities** for larger coupling.

(Resonance between localized internal mode and extended mode.)

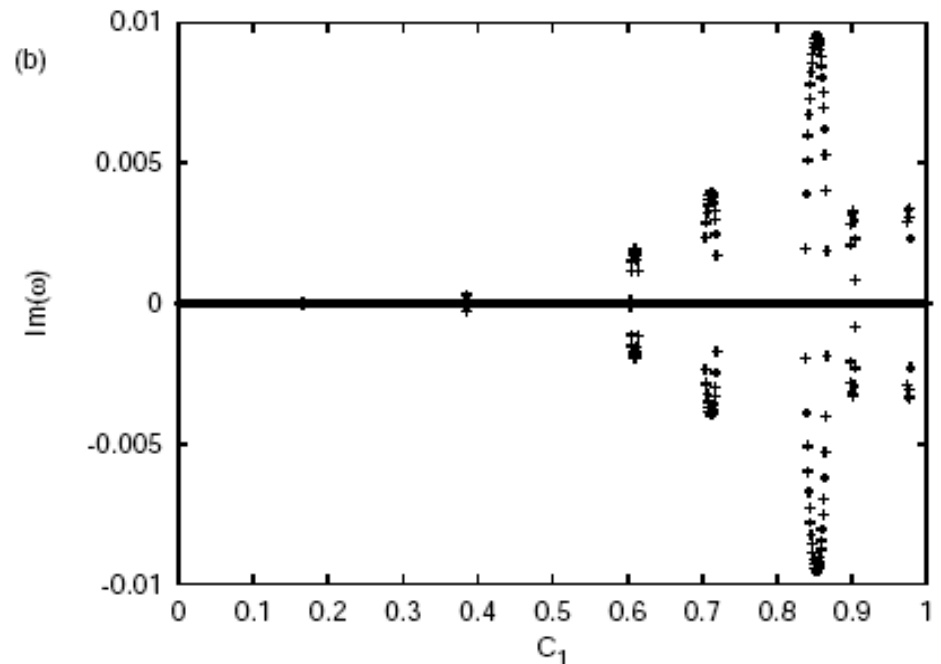
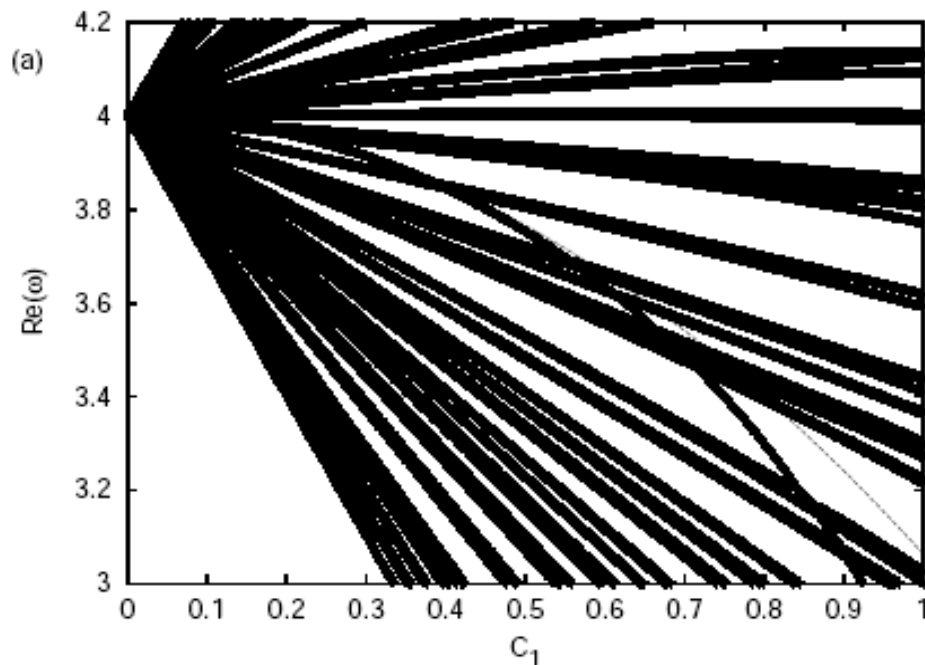
Analytical estimate for instability threshold obtained by calculating stability eigenvalues to order (C_1^2, C_2^2) .

In addition, all modes develop Vakhitov-Kolokolov (VK) “quasicollapse” instability close to continuum limit.

2. $\sigma/\gamma = 1/3$: (circular waveguides)

- Horizontal/vertical dipole modes (I) are **stable** and **diagonal** modes (II) **unstable** when $C_1 \neq C_2$: Lattice directions select favorable dipole orientations!
- Vortex modes (III) develop **weak oscillatory instabilities** for **any** values of the coupling when $C_1 \neq C_2$ if lattice is **infinite**.

For **finite** lattice: **Narrow windows** of very weak instabilities for small couplings.



(For $C_1 = C_2$ all modes remain marginally stable.)

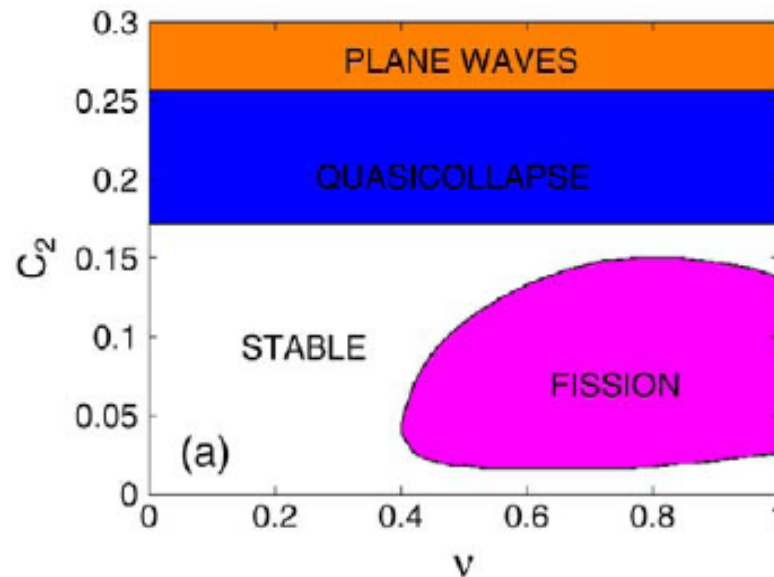
In addition, all modes develop VK instability close to continuum limit.

Directional mobility of dipole modes in square lattice:

Study of mobility for horizontal/vertical modes (I) reduces to **one-component anisotropic DNLS** (e.g. Kevrekidis et al., Phys. Rev. E **72**, 046613 (2005)).

Stable solutions mobile in the strong-coupling direction are known to exist for

$$C_2/C_1 \lesssim 0.17:$$



J. Gómez-Gardeñes et al. / Physica D 216 (2006) 31–43

(For vortices (III), no stable mobile solutions exist.)

Triangular lattice:

(cf. eg. Kevrekidis et al., PRE **66**, 016609 (2002); Koukouloyannis/MacKay, J. Phys. A **38**, 1021 (2005) for results on discrete solitons and vortices in 1-component models)

V Koukouloyannis and R S MacKay

$$i \frac{dA_{m,j}}{dz} - C_2(A_{m,j+1} + A_{m,j-1})$$

$$-C_{AA}(A_{m+1,j} + A_{m-1,j} + A_{m+1,j+1} + A_{m-1,j-1})$$

$$-C_{AB}(B_{m+1,j} + B_{m-1,j} - B_{m+1,j+1} - B_{m-1,j-1})$$

$$+\gamma|A_{m,j}|^2 A_{m,j} + \sigma (2|B_{m,j}|^2 A_{m,j} + B_{m,j}^2 A_{m,j}^*) = 0,$$

$$i \frac{dB_{m,j}}{dz} + C_1(B_{m,j+1} + B_{m,j-1}) - C_{BB}(B_{m+1,j} + B_{m-1,j} + B_{m+1,j+1} + B_{m-1,j-1})$$

$$-C_{AB}(A_{m+1,j} + A_{m-1,j} - A_{m+1,j+1} - A_{m-1,j-1}) + \gamma|B_{m,j}|^2 B_{m,j} + \sigma (2|A_{m,j}|^2 B_{m,j} + A_{m,j}^2 B_{m,j}^*) = 0.$$

$C_1 > 0$, $C_2 > 0$, $C_{AB} > 0$, sign of C_{AA} and C_{BB} depend on particular geometry.

Relation between coupling constants for circular waveguides ($\sigma/\gamma = 1/3$):

$$C_{AA} = \frac{1}{4} (C_2 - 3C_1) \quad (\text{valid more generally for waveguides having the same (6-fold) rotational symmetry as the lattice, or higher})$$

$$C_{AB} = \frac{\sqrt{3}}{4} (C_2 + C_1)$$

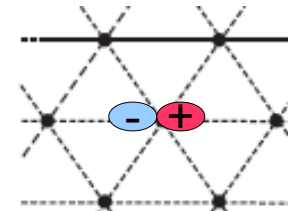
$$C_{BB} = \frac{1}{4} (3C_2 - C_1)$$

6-fold rotational symmetry \rightarrow

3 classes of distinct fundamental solutions appear from anticontinuous limit:

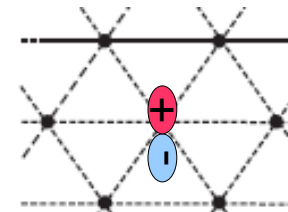
(i) Dipoles pointing **in lattice direction** (e.g. $B = 0$):

Stable when $C_2 > C_1$ (VK instabilities close to continuum limit).



(ii) Dipoles pointing **between lattice directions** (e.g. $A = 0$):

Stable when $C_2 < C_1$ (VK instabilities close to continuum limit).



In both cases, stability eigenvalues $\omega \sim (C_1^3, C_2^3)$.

(iii) **Vortex modes**: $B_{m_0, j_0} = \mp i A_{m_0, j_0}$; always (weakly) **oscillatorily unstable**.

(When $C_2 = C_1$, type (i) modes are stable for $\gamma = +1$ and type (ii) modes stable for $\gamma = -1$.)

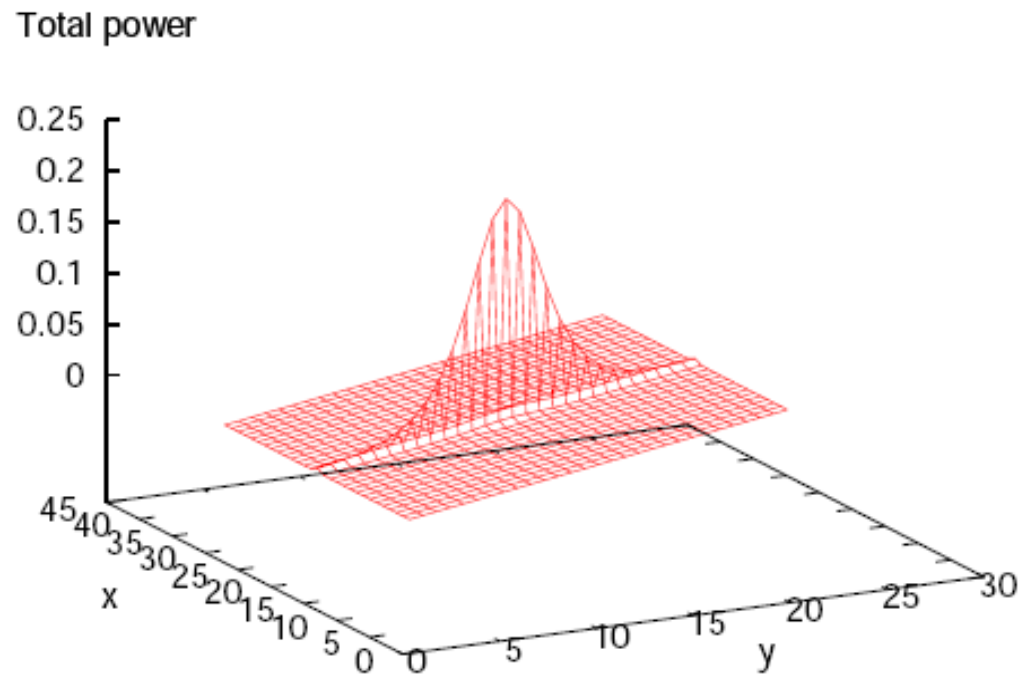
But the instability is very weak close to anticontinuous limit: $\omega/\beta \sim (C/\beta)^{13/2}$!!)

Directional mobility of dipole modes in triangular lattice:

Appears close to special parameter values where **VK-instabilities are suppressed**:

$$C_2 = C_1/3 \ (\rightarrow C_{BB} = 0), \ \gamma = +1, \ \text{and} \ C_2 = 3C_1 \ (\rightarrow C_{AA} = 0), \ \gamma = -1.$$

At these values, for large coupling the stable dipole mode approaches a **one-dimensional** band-edge mode in strong-coupling direction, and becomes **mobile** in this direction.



“Translational and Rotational mobility” of dipole modes:

Wellknown approach to measure **mobility** of discrete modes:
(Kivshar/Campbell, PRE **48**, 3077 (1993))



Calculate **energy difference at fixed power** between “one-site” and “two-site” modes:
“Peierls-Nabarro (PN) potential barrier”

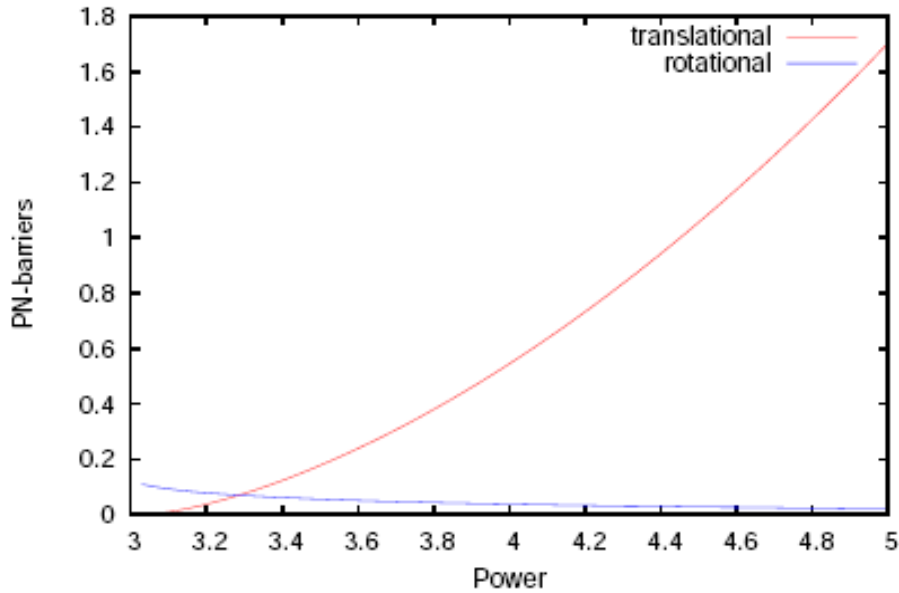
Analogously, we may define “**rotational PN barrier**” as energy difference between **stable** and **unstable** dipole modes →

Minimum energy needed for **rotation** of stable dipole modes!

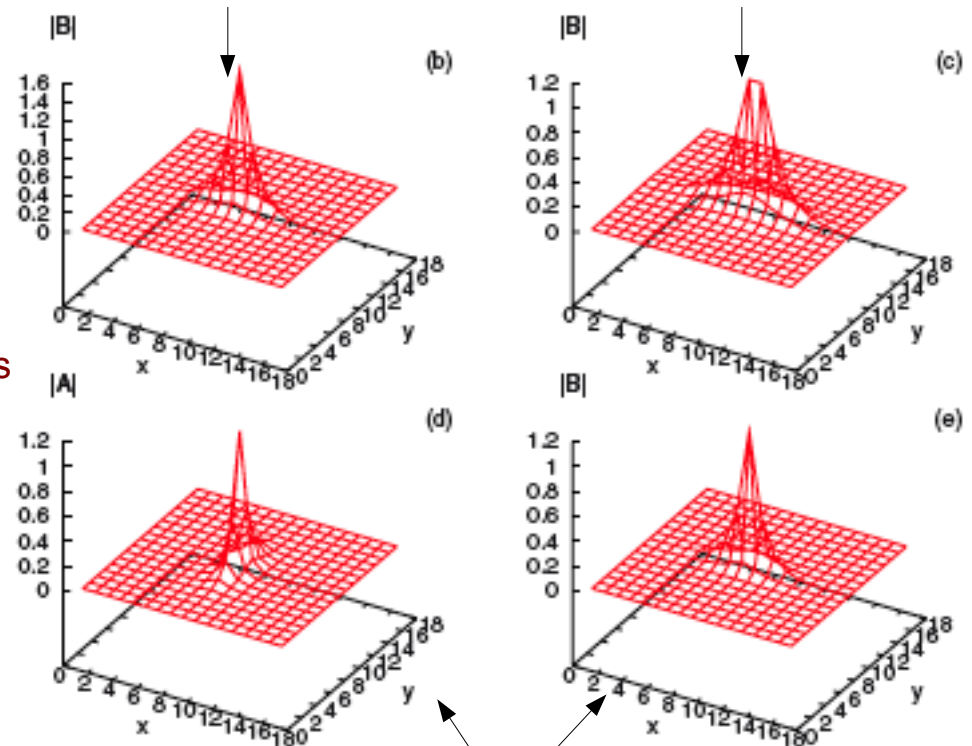
Comparison between translational and rotational barriers for square lattice:

Good mobility regime:

Square, $\sigma=1/3$, $C_2/C_1 = 0.15$



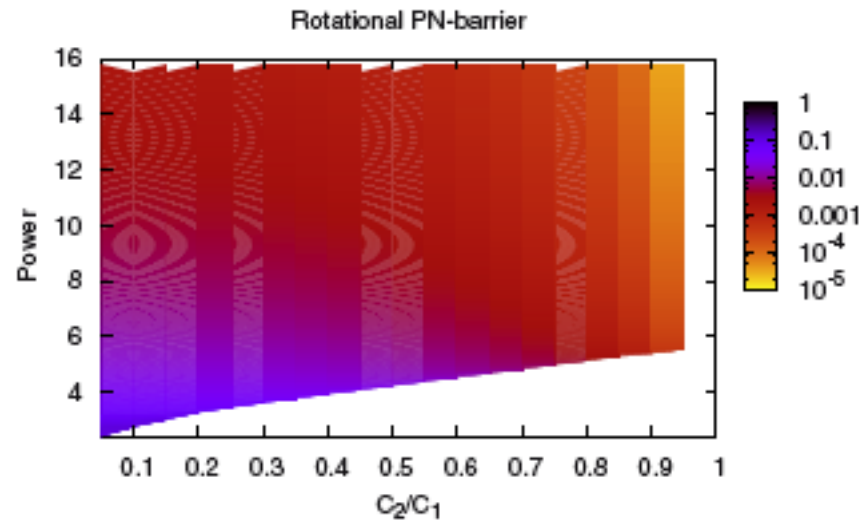
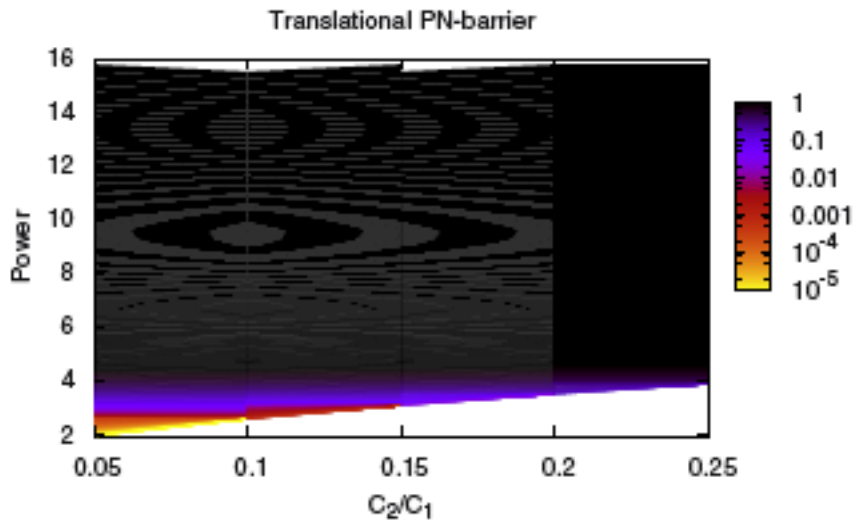
stable 1-site vertical mode ($A=0$) unstable 2-site vertical mode



dipole modes at $P \approx 3.28$:

unstable 1-site diagonal mode

General pictures for increasing power:
translational barrier increases, rotational decreases:



Dynamical illustration of rotational PN-barrier:

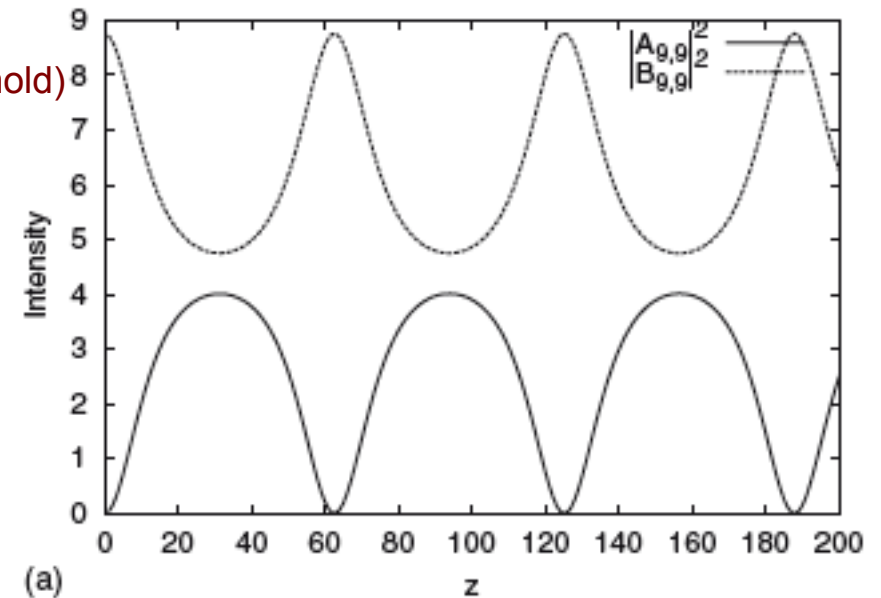
Perturbed stable 1-site vertical mode:

$\epsilon = 0.0112$ (just below rotation threshold)

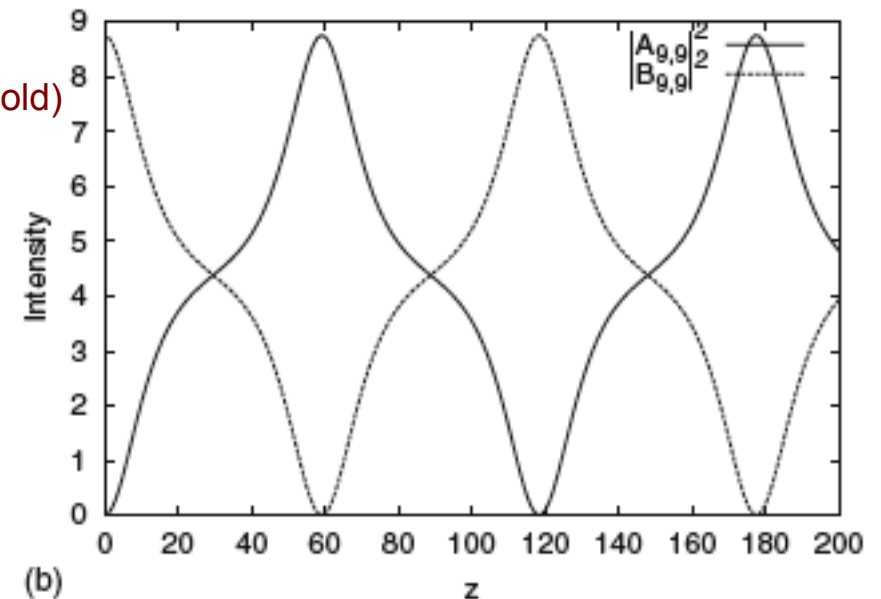
$$A'_{m,j} = A_{m,j} \cos \epsilon + iB_{m,j} \sin \epsilon,$$

$$B'_{m,j} = B_{m,j} \cos \epsilon + iA_{m,j} \sin \epsilon.$$

Central site intensity:

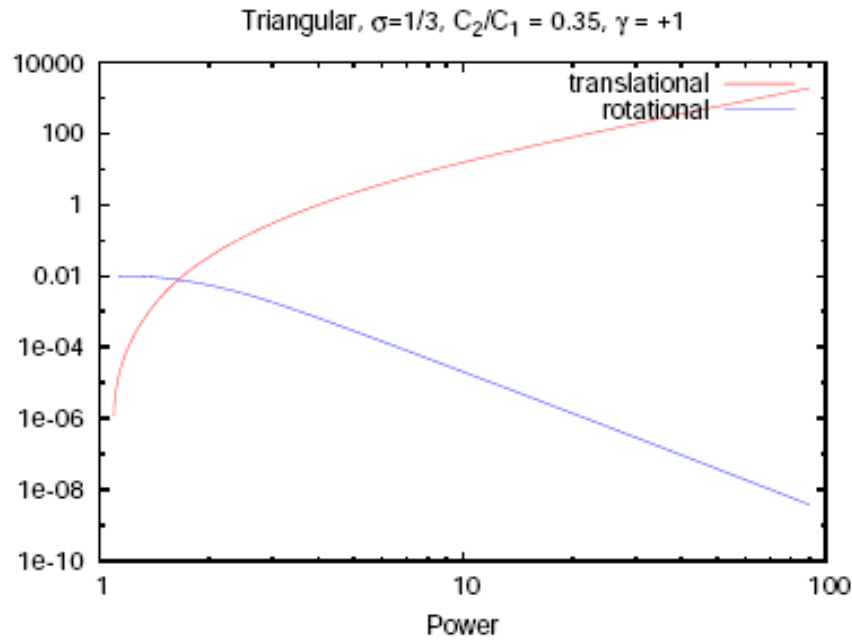


$\epsilon = 0.0113$ (just above rotation threshold)



Comparison between translational and rotational barriers for triangular lattices ($\gamma = +1$):

Good mobility regime:

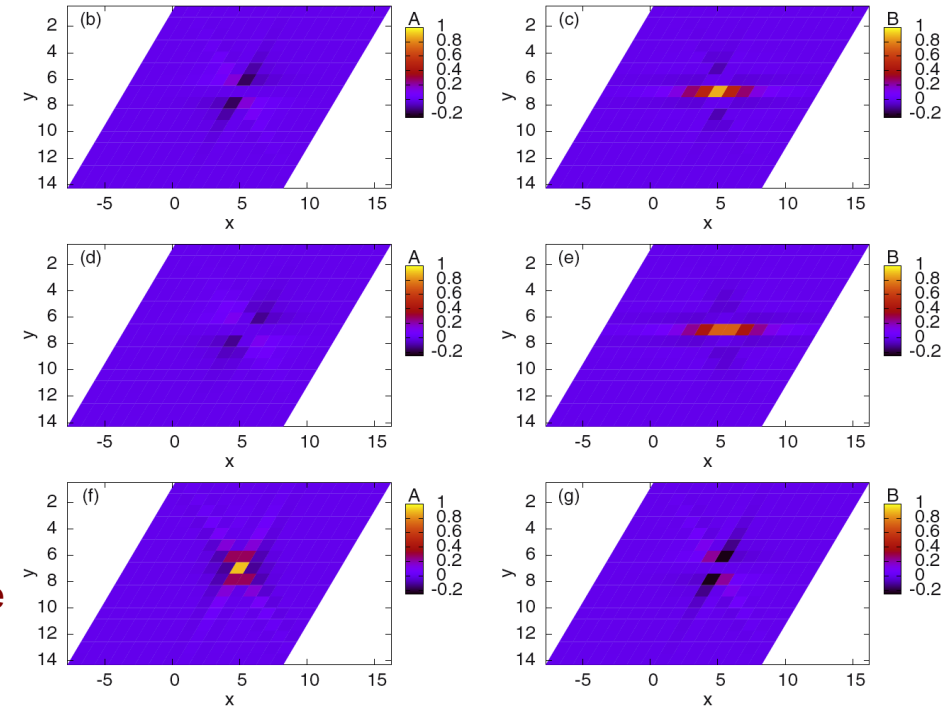


stable 1-site
vertical mode

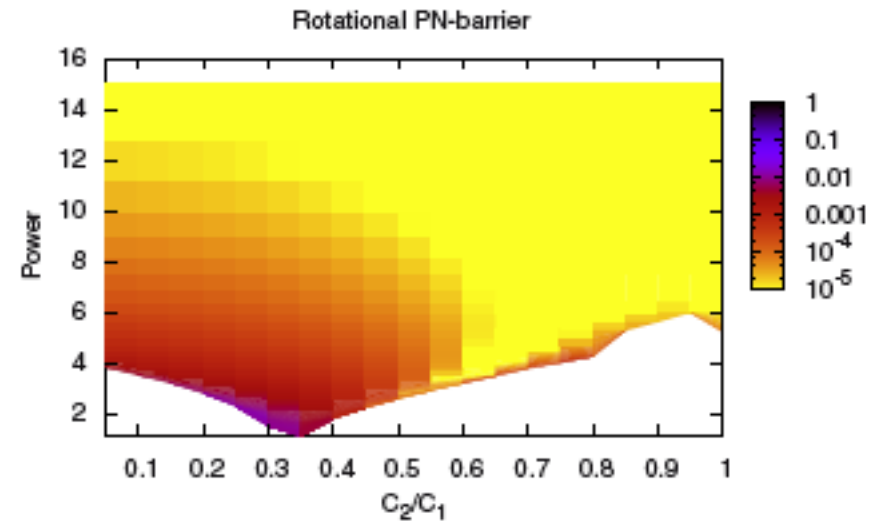
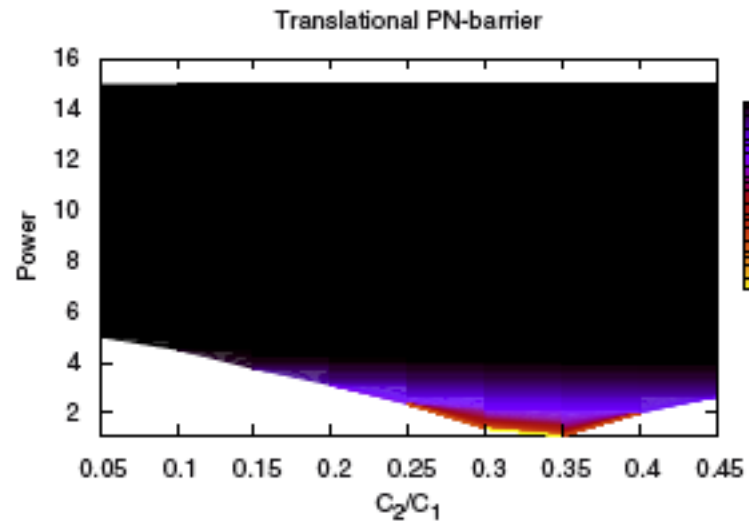
unstable 2-site
vertical mode

unstable 1-site
horizontal mode

dipole modes at $P \approx 1.65$:



General pictures:



Dynamical illustration of rotational PN-barrier for triangular lattice:

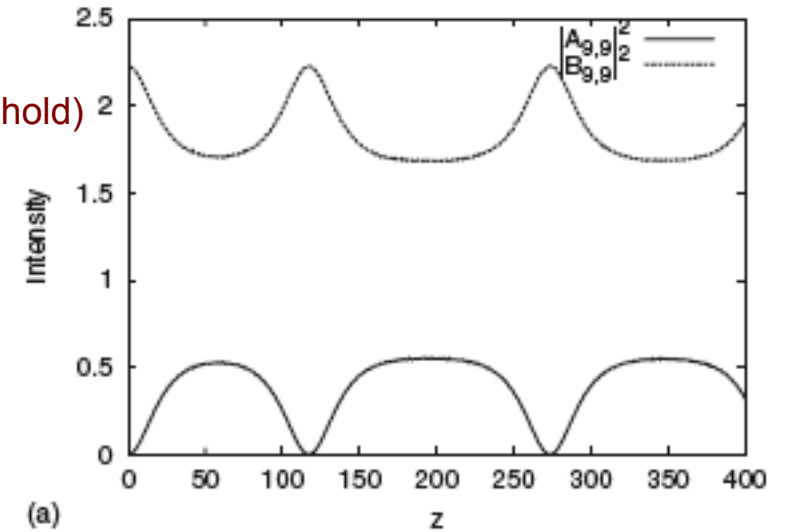
Perturbed stable 1-site vertical mode:

$$A'_{m,j} = A_{m,j} \cos \epsilon + iB_{m,j} \sin \epsilon,$$

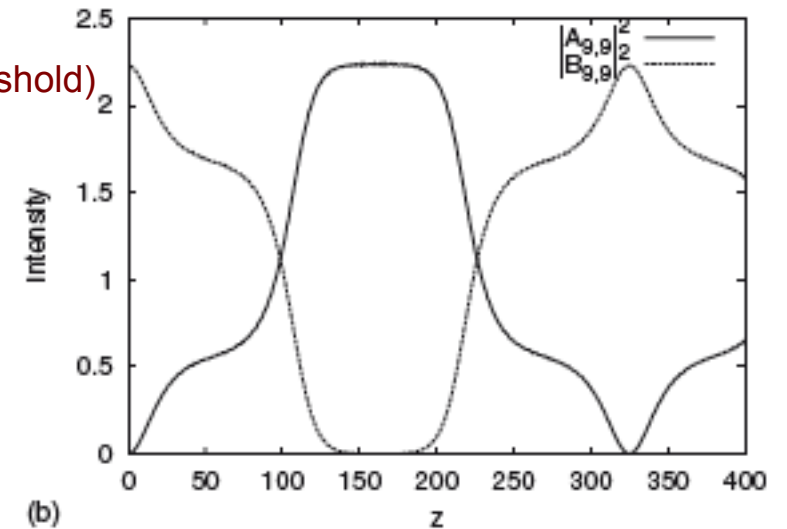
$$B'_{m,j} = B_{m,j} \cos \epsilon + iA_{m,j} \sin \epsilon.$$

$\epsilon = 0.0306$ (just below rotation threshold)

Central site intensity:



$\epsilon = 0.0307$ (just above rotation threshold)



Note: first barrier to overcome is unstable solution rotated 30° , with $|B|^2 = 3|A|^2$ at central site.

Dynamical illustration of translational PN-barrier for triangular lattice:

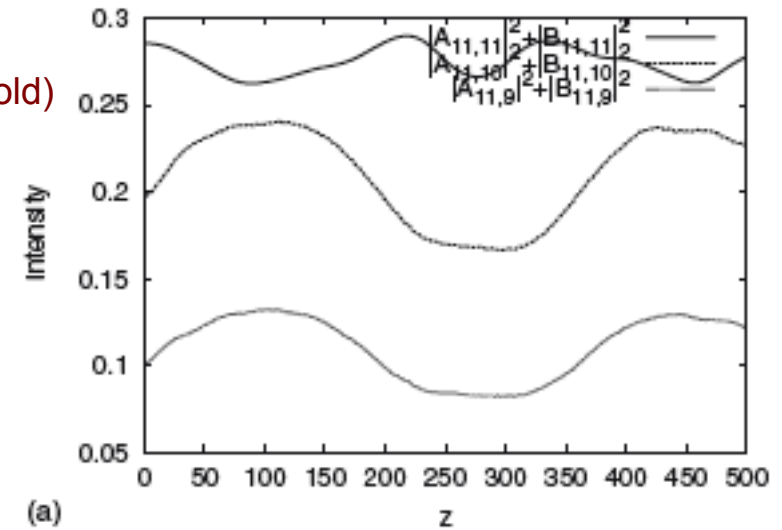
Perturbed stable 1-site vertical mode:

$$A'_{mj} = A_{mj} \exp(-i\epsilon j),$$

$$B'_{mj} = B_{mj} \exp(-i\epsilon j).$$

$\epsilon = 0.012$ (just below translation threshold)

Intensity of central site
+ 2 horizontal neighbours:



$\epsilon = 0.014$ (just above translation threshold)

